AGU PUBLICATIONS

JGR

Journal of Geophysical Research: Space Physics

RESEARCH ARTICLE

10.1002/2014JA020410

Key Points:
- DEMETER has observed bursty MF waves in the auroral ionosphere
- The MF waves resemble MF burst observed at ground level
- Current theories of MF burst generation should account for in situ observations

Correspondence to:
M. C. Broughton,
matthew.broughton.gr@dartmouth.edu

Citation:
Broughton, M. C., J. LaBelle, and M. Parrot (2014), DEMETER observations of bursty MF emissions and their relation to ground-level auroral MF burst, *J. Geophys. Res. Space Physics*, *119*, 10,144–10155, doi:10.1002/2014JA020410.

Received 19 JUL 2014
Accepted 28 OCT 2014
Accepted article online 30 OCT 2014
Published online 1 DEC 2014

DEMETER observations of bursty MF emissions and their relation to ground-level auroral MF burst

M. C. Broughton[1], J. LaBelle[1], and M. Parrot[2]

[1]Department of Physics and Astronomy, Dartmouth College, Hanover, New Hampshire, USA, [2]LPC2E, CNRS, Orléans, France

Abstract A survey of medium frequency (MF) electric field data from selected orbits of the Detection of Electro-Magnetic Emissions Transmitted from Earthquakes (DEMETER) spacecraft reveals 68 examples of a new type of bursty MF emissions occurring at high latitudes associated with auroral phenomena. These resemble auroral MF burst, a natural radio emission observed at ground level near local substorm onsets. Similar to MF burst, the bursty MF waves observed by DEMETER have broadband, impulsive frequency structure covering 1.5–3.0 MHz, amplitudes of 50–100 μV/m, an overall occurrence rate of ~0.76% with higher occurrence during active times, and strong correlation with auroral hiss. The magnetic local time distribution of the MF waves observed by DEMETER shows peak occurrence rate near 18 MLT, somewhat earlier than the equivalent peak in the occurrence rate of ground level MF burst, though propagation effects and differences in the latitudes sampled by the two techniques may explain this discrepancy. Analysis of solar wind and SuperMAG data suggests that while the bursty MF waves observed by DEMETER are associated with enhanced auroral activity, their coincidence with substorm onset may not be as exact as that of ground level MF burst. One conjunction occurs in which MF burst is observed at Churchill, Manitoba, within 8 min of MF emissions detected by DEMETER on field lines approximately 1000 km southeast of Churchill. These observations may plausibly be associated with the same auroral event detected by ground level magnetometers at several Canadian observatories. Although it is uncertain, the balance of the evidence suggests that the bursty MF waves observed with DEMETER are the same phenomenon as the ground level MF burst. Hence, theories of MF burst generation in the ionosphere, such as beam-generated Langmuir waves excited over a range of altitudes or strong Langmuir turbulence generating a range of frequencies within a narrow altitude range, need to be revisited to see whether they predict in situ detection of MF burst.

1. Introduction

The auroral ionosphere is a rich source of plasma waves that can be observed in space and at ground level. The latter case includes auroral medium frequency burst (first reported by *Weatherwax et al.* [1994]), which is an impulsive, broadband natural radio emission that occurs from 1.3 to 4.5 MHz and is often observed at ground level near local substorm onset. It is left-hand polarized [*Shepherd et al.*, 1997], predominately occurs in the 4 h preceding magnetic midnight [*LaBelle et al.*, 1997] and has a direction of arrival that follows the motion of the poleward edge of an auroral arc [*Bunch et al.*, 2008, 2009]. Using continuous waveform measurements, *Bunch and LaBelle* [2009] reported that MF burst consists of both structured and unstructured features, with structured features accounting for 30–40% of the wave power. *LaBelle* [2011] proposed that MF bursts originate as Langmuir/*Z*-mode waves on the topside of the ionosphere that mode convert to *L*-mode waves and propagate to ground level. Recently, *Akbari et al.* [2013] presented an example of coherent echoes measured by the Poker Flat Incoherent Scatter Radar that occurred at the same time when MF bursts were observed at Toolik Lake, Alaska, leading the authors to propose that both the coherent echoes and the MF bursts could be manifestations of the same ionospheric process. There have been comparisons between ground level MF burst measurements and particle data from low-altitude satellites [*Sato et al.*, 2008; *LaBelle et al.*, 2009]. However, there have been no simultaneous observations of MF bursts at ground level and by nearby spacecraft, even though there have been multiple observations of broadband MF emissions from low-altitude satellites in the morning auroral oval [*Shutte et al.*, 1997] and in the topside cusp ionosphere [*Rothkaehl*, 1999].

Observations of broadband MF waves in the topside connected to MF burst would be significant for several reasons. Despite their close connection with substorm onset and possible use for timing and locating

©2014. American Geophysical Union. All Rights Reserved.

substorm onsets, the underlying cause of MF burst emissions remains controversial. One suggested mechanism, involving mode conversion of Langmuir waves in the topside *F* region [*LaBelle*, 2011], predicts emanation of *O*-mode waves with characteristics very similar to MF burst into the topside. Detection of topside MF waves connected to MF burst would confirm this prediction and test predictions of other generation mechanisms. The possibility to study MF burst from an in situ platform would inspire experiments to measure electron distribution functions associated with MF burst, which would comprise the most definitive test of the generation mechanism. Topside observations of MF waves do not suffer from *D* region absorption, which severely limits what can be learned about MF burst from ground level. For example, ground level observations suggest a connection between MF burst and the poleward expanding auroral arc during substorm onset, but absorption effects make it impossible to prove the connection, whereas topside observations unaffected by absorption might be used to establish such a connection. Finally, the topside generation mechanism of MF burst [*LaBelle*, 2011] predicts that the frequency structure of the emissions can be used to remotely sense the topside density profile, and application of this technique would provide a new tool for in situ experiments.

Parrot et al. [2009] performed a global study of MF emissions observed by the low-altitude Detection of Electro-Magnetic Emissions Transmitted from Earthquakes (DEMETER) spacecraft. Many of the MF waves in that study were observed near very low frequency (VLF) ground-based transmitters and were interpreted to be lightning-induced MF waves that propagated to satellite altitudes via ionospheric perturbations associated with the transmitters. These are almost certainly unrelated to MF burst. However, there was a population of waves [see *Parrot et al.*, 2009, Figure 3] that occurred at similar range of invariant latitudes as those at which MF bursts are typically observed. The following study describes these MF waves observed with DEMETER and explores the possible relationship, if any, between the bursty MF waves observed by DEMETER at high latitudes and auroral medium frequency burst.

2. Instrumentation

The Detection of Electro-Magnetic Emissions Transmitted from Earthquakes (DEMETER) satellite was launched in June 2004 in a circular polar orbit at an altitude of 720 km. In 2005, the orbital altitude was changed to approximately 670 km. The spacecraft's orbit was Sun synchronous, with each orbit consisting of a dayside (~10:30 MLT) and nightside (~22:30 MLT) half orbit. Under normal operations, the spacecraft did not record data above 65° invariant latitude. However, on select orbits, the spacecraft did record data at high latitudes, often in conjunction with ionospheric heater operations at HAARP in Alaska or Eiscat in Norway.

DEMETER wave measurements were made by the Instrument Champ Electrique (ICE) instrument. A full description of the instrument can be found in *Berthelier et al.* [2006]. The instrument consists of four spherical sensors, along with embedded preamplifiers that were mounted at the end of four stacer arms with a length of 4 m. To determine the electric field along an axis defined by two sensors, the instrument measured the potential difference between the two sensors. Since this can be done with any pair of sensors, the instrument could measure three components of the electric field in certain frequency ranges. For the ULF (0–15 Hz) channel, continuous waveform measurements were made of three components of the electric field. For the VLF (15 Hz–20 kHz) channel, data from one component of the electric field were digitized with 16 bits at 40 kHz and Fourier transformed with a 19.53 Hz resolution. Forty spectra were averaged to provide a survey spectrogram every 2.048 s. For the HF (3.25 kHz–3 MHz) channel, data from one component of the electric field were digitized with 8 bits at 6.66 MHz for a snapshot 0.6144 ms in length. Each snapshot was Fourier transformed, and the resultant power spectra were averaged to create a survey spectrograms with 3.25 kHz resolution every 2.048 s. During certain periods, longer waveform snapshots were recorded.

Ground level data were inspected from two radio observation sites: Toolik Lake, Alaska (68°38′N, 211°24′W, invariant latitude 68.51°N) and Churchill, Manitoba (58°45′47″N 266°56′12″E, invariant latitude 69.2°N). All measurements were made using a 10 m^2 magnetic loop antenna with a preamplifier located at the base of the antenna in a weatherproof PVC case. The signals from the preamplifier were transmitted via coaxial cable to one of two receivers. At Churchill, the signals were transmitted to a programmable receiver, which swept from 0.03 to 5 MHz in 10 kHz steps every 2 s. The wave intensity at each frequency was recorded by a computer. A full description of the experimental equipment is presented in *Weatherwax* [1994]. At Toolik Lake, the signals were transmitted to a receiver that band-pass-filtered the data between 100 kHz and 5 MHz and controlled the signal level with an automatic gain control. The signals were then digitized with 12 bit

©2014. American Geophysical Union. All Rights Reserved.

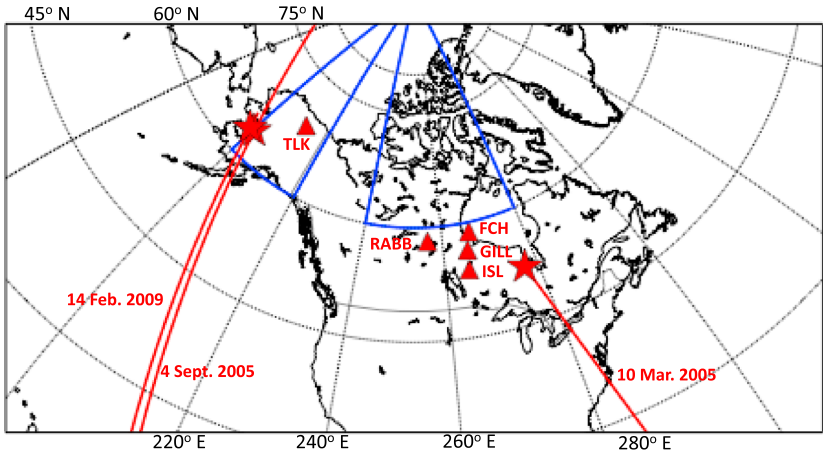

Figure 1. A map showing DEMETER orbits for the three examples shown in the paper. The stars indicate when DEMETER observed bursty MF waves. Also shown are the locations of Toolik Lake (TLK), Churchill (FCH), Island Lake (ISL), Gillam (GILL), and Rabbit Lake (RABB). The blue lines outline the regions used in the half orbit selection.

resolution at 10 MHz by an analog-to-digital converter. Waveform snapshots of 98,304 points were recorded every 2 s for 23.5 h each day. Data were reviewed shortly after collection. Raw data from intervals containing natural radio emissions were saved, whereas only summary spectrograms were saved for intervals not containing natural radio emissions. A full description of this system is presented in *Bunch* [2010].

3. Comparison of Satellite and Ground Level Data

3.1. Wave Characteristics

Inspired by Figure 3 of *Parrot et al.* [2009], a study was devised to characterize the high-latitude MF waves observed therein and determine whether they are associated with ground level MF burst. Summary spectrograms of nightside half orbits from DEMETER (http://demeter.cnrs-orleans.fr/) were selected for inspection if they met two criteria. First, the half orbit needed to occur between September and April, a period during which the high-latitude Northern Hemisphere was likely to be in darkness, a condition favorable to the propagation of MF waves to ground level because of the depleted electron density in the lower regions of the ionosphere. Second, during the half orbit, the spacecraft needed to pass through one of two geographic areas at some point in its orbit. The geographic latitude range of both areas was 60–90°N. The two geographic longitude ranges were 200–220°E or 240–280°E. These ranges were chosen to increase the probability that a selected orbit pass close to ground level radio observation sites at Toolik Lake and Churchill. Application of these criteria yielded 8624 half orbits. Visual inspection of summary spectrograms from these half orbits yielded 68 observations of bursty MF waves, which occurred on 66 separate half orbits. Figure 1 shows the two regions (blue outlines) and shows locations of three selected bursty wave events (red stars) as well as the DEMETER orbits pertaining to these (red lines). Also plotted are the locations of the Dartmouth observatories at Toolik Lake (TLK) and Churchill (FCH) as well as the locations of magnetometers at Island Lake (ISL, 53°51′21″N, 94°39′36″W), Gillam (GILL, 56° 27′30″N, 94° 12′30″W), and Rabbit Lake (RABB, 58°13′19″N, 103°40′48″W).

Figure 2 shows a typical example of bursty MF waves observed in HF, VLF, and ULF wave data recorded by DEMETER on 14 February 2009. During this time period, DEMETER was at an altitude of approximately 670 km, moving poleward in the Northern Hemisphere near 19:30 Magnetic Local Time (MLT). The red line in the top panel near 1 MHz is f_{ce} as determined by the IGRF 2000 magnetic field model with coefficients extrapolated from 2005. The bursty MF waves, indicated by an arrow in the figure, occurred from 7:28:40 to 7:33 UT at 1600–2600 kHz in the top panel, which is an HF frequency-time spectrogram covering 3 kHz–3 MHz. The power spectral density of the wave was modulated with an approximate period of 15 s as determined by visual inspection of the frequency-time spectrogram. This type of modulation occurred in nine of the 68 examples of MF emissions identified in this study.

Figure 2 (middle), a VLF frequency-time spectrogram covering 15 Hz–20 kHz, shows that an increase in VLF wave power occurred shortly before the appearance of the bursty MF waves and continued for a short time

©2014. American Geophysical Union. All Rights Reserved.

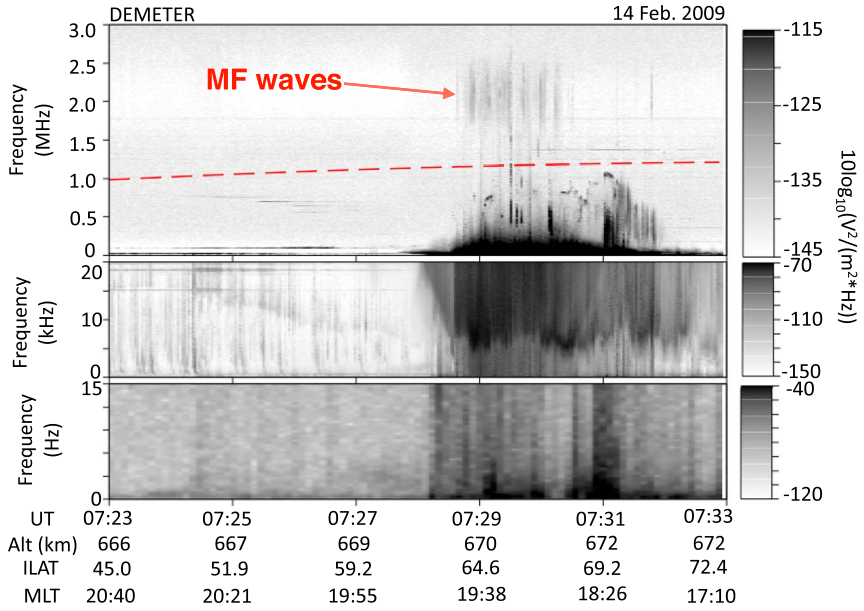

Figure 2. (top) A frequency-time spectrogram of one component of the HF electric field measured by DEMETER. Bursty MF waves are present from 7:28:40 to 7:33 UT. The red line is the f_{ce} *inferred from IGRF.* (middle) A frequency-time spectrogram of the VLF electric field. (bottom) A frequency-time spectrogram of the ULF electric field. Increases in VLF and ULF wave power are coincident with the bursty MF waves.

after the spacecraft ceased to observe the MF waves. The VLF waves can also be seen in Figure 2 (top), since they extend above the 3 kHz lower boundary of HF receiver. Similar VLF waves were observed at or near the same time as the bursty MF waves in all 68 events of this study. The VLF waves probably represent auroral hiss, a whistler-mode emission observed by low-altitude satellites on virtually every overpass of the aurora [e.g., *Gurnett et al.*, 1983] and often observed at ground level coincident with MF burst [e.g., *LaBelle et al.*, 1997]. The top panel of Figure 2 also shows narrow band waves at the top end of the range of the auroral hiss; these are probably Langmuir waves, which indicate that the local plasma frequency was below f_{ce}. Proposed mechanisms of MF burst emissions associate them with Langmuir waves. The bottom panel of Figure 2, a ULF spectrogram covering 0–15 Hz, shows that there was also an increase in power below 1 Hz at the same time that DEMETER observed the bursty MF waves, although it is unclear if this was due to spatial or temporal electric field variations. A similar increase in power below 1 Hz occurred in 57 of the 68 examples of MF waves identified in this study.

Figure 3, in the same format as Figure 2, shows another example of the MF waves observed by DEMETER at 1.7–2.5 MHz starting at 07:52:30 UT on 4 September 2005. During this period, DEMETER was moving poleward in the Northern Hemisphere in the premidnight/preevening sector. In this case, the satellite stopped data collection before it ceased to observe the waves. The bursty MF waves occurred at the same time as an increase in the power of the VLF waves, shown in Figure 3 (middle), but no increase in ULF wave power was observed. Similar to the previous event, narrow band Langmuir waves were visible near 0.75 MHz.

For each of the 68 examples of bursty MF waves observed by DEMETER, the power spectral density was integrated between the upper and lower frequency boundaries of the waves to give an electric field amplitude. The mean electric field strength was 100 μV/m with a standard deviation of 25 μV/m. For comparison, MF burst amplitudes measured at ground level tend to be 50–100 μV/m [*LaBelle et al.*, 1997]. The interpretation of the wave amplitudes contains some subtleties. First, neither the in situ nor ground level instruments operated at 100% duty cycle. *Bunch et al.* [2009] showed that fine structure features lasting 10–100 ms account for 30–40% of the MF burst wave power spectral density [*LaBelle and Treumann*, 2002]. Instruments with a low duty cycle would not resolve these fine structures, thus underestimating the power. Since the satellite and ground level measurements had the same time resolution, the time resolution is presumably not a problem when comparing the two power spectral densities. Second, both the in situ and ground level measurements were of only one component of the wave field. This most likely contributed little to uncertainty in the estimation of the wave power spectral density. The ground level measurements cited above were

©2014. American Geophysical Union. All Rights Reserved.

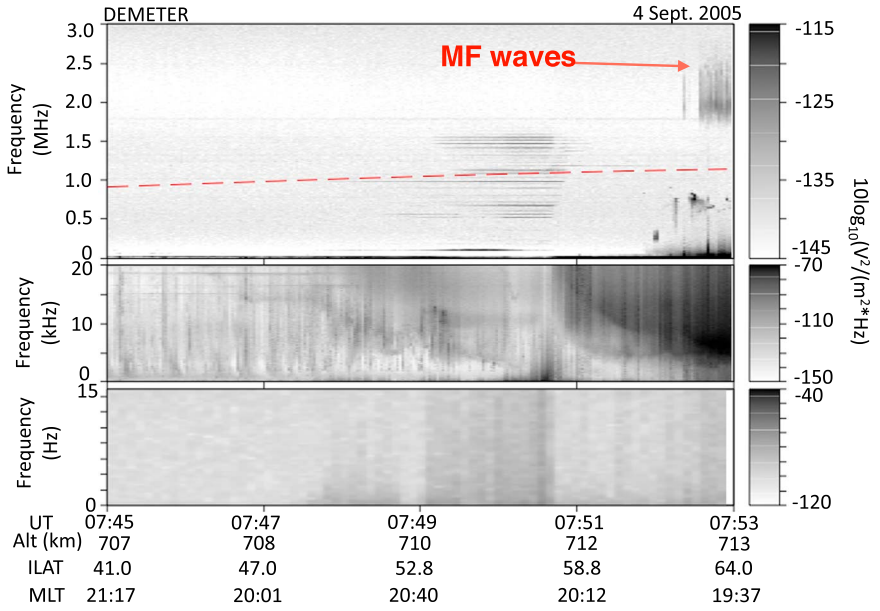

Figure 3. A frequency-time spectrogram of (top) HF, (middle) VLF, and (bottom) ULF electric fields measured by DEMETER, in the same format as Figure 2. Bursty MF waves occur starting at 07:52:21. An increase in VLF wave power coincides with the bursty MF waves.

made with a vertical magnetic loop antenna. Therefore, the ground level estimates of wave amplitude are fairly accurate, assuming the waves are circularly or elliptically polarized and propagate from approximately overhead. On DEMETER, all HF electric field measurements were along the *Y* axis of the spacecraft, which pointed approximately in the east-west direction in the Northern Hemisphere. If we assume that the waves measured by the satellite were elliptically or circularly polarized electromagnetic waves, the angle between the *Y* axis of the spacecraft and the electric field of the waves was probably small and would have little effect on the amplitude measurements.

Figure 4a shows the distribution of MLT values for the bursty MF emissions observed by DEMETER (red) and for MF bursts observed at Churchill (blue). The vertical axis is the number of events in each MLT bin divided by the total number of events. The Churchill MF bursts came from a database of 873 MF bursts observed at Churchill from 1994 to 2009 [*LaBelle et al.*, 2009]. The error bars represent 2 standard deviations as defined by counting statistics. The distribution of MF burst MLT values peaks at 22 MLT, and the distribution of MLT values for the DEMETER bursty MF emissions peaks near 18 MLT. A direct comparison between the two histograms is difficult. The observations at Churchill uniformly spanned all MLTs. In contrast, DEMETER's Sun-synchronous orbit caused it to spend more time in certain magnetic local time sectors. In order to better compare the two distributions, the histogram of Churchill MF bursts was multiplied by a weighting function derived from the MLT distribution of DEMETER orbits. Roughly speaking, the effect of this is to present an MLT distribution of MF burst that one would expect to see by DEMETER given both the distribution of magnetic local time of MF burst and the orbital coverage of DEMETER. The results of this are shown in Figure 4c. This convolved distribution of MF burst MLT values peaks near 21 MLT, still somewhat later than that of the peak in the distribution of DEMETER MF wave observations.

Figures 4b and 4d show the distribution of lower and upper frequency boundaries of the bursty MF emissions observed by DEMETER and those of the 873 MF bursts observed at Churchill from 1994 to 2009. The DEMETER observations were restricted to below 3 MHz, whereas the frequency distribution of ground level MF burst is bimodal, with occurrences below and above 3 MHz [see *Weatherwax et al.*, 1994, Figure 2]. (On those occasions when ground level MF burst spans both below and above 3 MHz, a null is often observed at 3 MHz.) Therefore, only those Churchill MF bursts with an upper frequency boundary below 3 MHz were included in Figure 4d. The median lower frequency boundary was 1660 kHz for the DEMETER bursty MF waves and 1810 kHz for the Churchill MF bursts. The median upper frequency boundary was 2630 kHz for the DEMETER bursty MF waves and 2620 kHz for the Churchill MF bursts.

©2014. American Geophysical Union. All Rights Reserved.

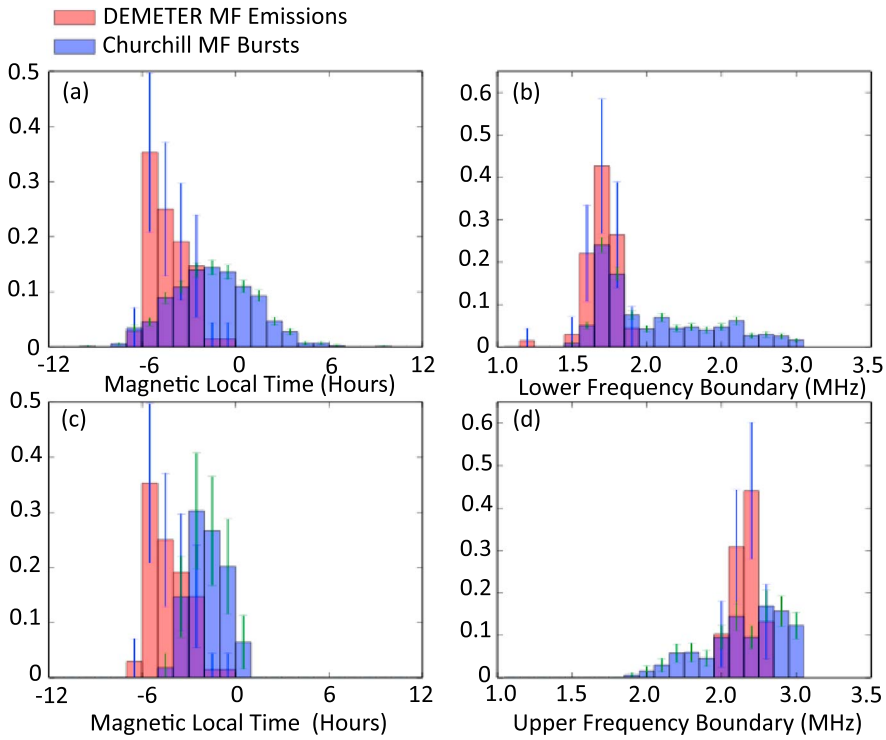

Figure 4. (a) The distribution of MLT of the bursty MF waves observed by DEMETER (red) and 873 MF bursts observed at Churchill (blue). (b) The distribution of lower frequency boundaries of the bursty MF waves observed by DEMETER (red) and MF bursts observed at Churchill (blue). (c) The distribution of MLT of the bursty MF waves observed by DEMETER (red) and MF bursts observed at Churchill convolved with the DEMETER MLT orbital coverage (blue). (d) The distribution of upper frequency boundaries of the bursty MF waves observed by DEMETER (red) and MF bursts observed at Churchill (blue). In each histogram, the vertical axis is the number of events in each bin normalized by the total number of events.

3.2. Conjunction Studies

Thirty-nine of the 68 bursty MF events occurred during times when data were recorded at Toolik Lake (for bursty MF waves observed over Alaska) or Churchill, Manitoba (for waves observed over Canada). Twenty-five of these bursty MF waves occurred within 1000 km ground distance of one of the Dartmouth HF radio observatories, and 15 occurred within 600 km. For reference, ground level observations at multiple observatories have seen MF burst observed by antennas separated by as much as 600 km [*LaBelle et al.*, 2005]. Within this data set, there was one case in which similar waves were observed by DEMETER and by a radio receiver at ground level.

Figure 5 shows details of this single conjunction event. The top two panels of Figure 5 are frequency-time spectrograms of data from DEMETER (Figure 5a) and Churchill (Figure 5b). DEMETER observed bursty MF waves at 1600–2500 kHz shortly before 3:08 UT on 10 March 2005. At the time DEMETER observed the waves, it was located approximately 1000 km southeast of Churchill, Manitoba. An MF burst in a similar frequency range occurred near 3:15 UT at Churchill, as can be seen in Figure 5b. The narrowband emission near 2.8 MHz in Figure 5b is auroral roar, a natural radio emission that occurs near harmonics of the ionospheric electron cyclotron frequency [*Kellogg and Monson*, 1979]. There is evidence for a second, weaker MF burst at a somewhat higher frequency (2.5–2.8 MHz) observed at Churchill at approximately 03:24–03:26 UT. During this 0313 UT MF burst event, the local Churchill magnetometer showed no significant (>50 nT) drop in the horizontal (*H*) component, as would be expected for a local substorm onset. However, activity was observed on magnetometers located at Gillam, Island Lake, and Rabbit Lake. As can be seen in Figure 1, Gillam and Island Lake are located south of Churchill along the same magnetic meridian, and Rabbit Lake is located west and slightly south of Churchill. Figure 5c shows a plot of the *H* component of the magnetic field from these three sites. In order to display all three on the same plot, an offset, given in the legend of the plot, was subtracted from the *H* component at each site. The vertical red line indicates when DEMETER observed bursty MF waves, and the vertical blue line indicates when the Churchill receiver observed bursty

©2014. American Geophysical Union. All Rights Reserved.

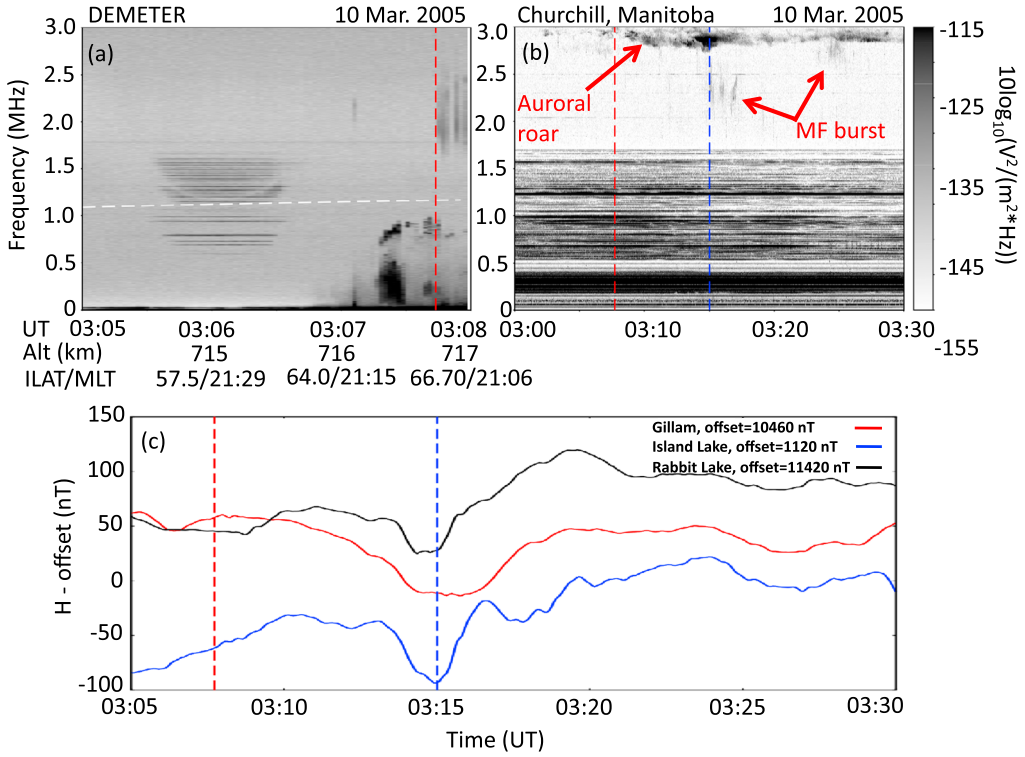

Figure 5. (a) A frequency-time spectrogram of one component of the HF electric field measured by DEMETER. The white dashed line indicates f_{ce}. Bursty MF waves were present starting at 3:07:44 UT, indicated by the dashed red line. (b) A frequency-time spectrogram from a ground level antenna located at Churchill Manitoba. An MF burst was observed near 3:15 UT, indicated by the vertical dashed blue line. (c) The horizontal component of the magnetic field, with an offset subtracted, measured at Gillam (red), Island Lake (blue), and Rabbit Lake (black). All three sites show a decrease in the *H* component near the time the MF burst was observed at Churchill.

MF waves. Decreases in the *H* component were observed at all three sites near the time when the MF burst was observed at Churchill, approximately 7 min after DEMETER observed bursty MF waves.

Other magnetometers operating in the Northern Canada sector (Dawson City, Contwoyto, Fort Smith, and Fort Simpson) showed no evidence of substorm activity. Cloudy skies prevented use of optical measurements at Gillam and Rankin Inlet to confirm substorm activity.

3.3. Association With Auroral Activity

Figure 6 (top) shows the results of a superposed epoch analysis of solar wind data, obtained from the OMNI database [*Qin et al.*, 2007]. The analysis used three different epoch times: the onset of the DEMETER bursty MF waves (red trace), the onset of MF bursts at Churchill (blue trace), and random epochs (black trace). The vertical axis, which is the median of the rate magnetic flux, is opened at the magnetopause: $\frac{d\phi_{MP}}{dt} = v^{4/3}(B_T)^{2/3}\ \sin(\theta_c/2)^{8/3}$, where v is the solar wind velocity; $B_T = \sqrt{B_y^2 + B_z^2}$; and θ_c is the solar wind clock angle. *Newell et al.* [2007] proposed this function as a proxy for the dayside merging rate and found that it was strongly correlated with auroral activity. For reference, when averaged over a solar cycle $\frac{d\phi_{MP}}{dt} = 4421\ (\mathrm{km/s})^{4/3}\ (\mathrm{nT})^{2/3}$. The shaded areas show the bootstrapped 95% confidence interval of the median. Both the DEMETER bursty MF emissions and the Churchill MF bursts are associated with an increase in $\frac{d\phi_{MP}}{dt}$ preceding the events. The value of $\frac{d\phi_{MP}}{dt}$ is greater for the DEMETER bursty MF waves and occurs over a longer time interval. The random epochs show no effect as expected.

Figure 6 (bottom) shows the results of the superposed epoch analysis of the SML index (a generalization of the *AL* index) derived from SuperMAG data. (For a description of the SML index and its relationship to substorms, see *Gjerloev* [2009] and *Newell and Gjerloev* [2011].) Figure 6 (bottom) shows the results of superposed epoch analyses of the SML index where the epoch times were taken to be the time when DEMETER observed MF waves (red line), the time when MF bursts were observed at Churchill (blue line), and random times (black line). The shaded areas show the bootstrapped 95% confidence interval of the median. The

©2014. American Geophysical Union. All Rights Reserved.

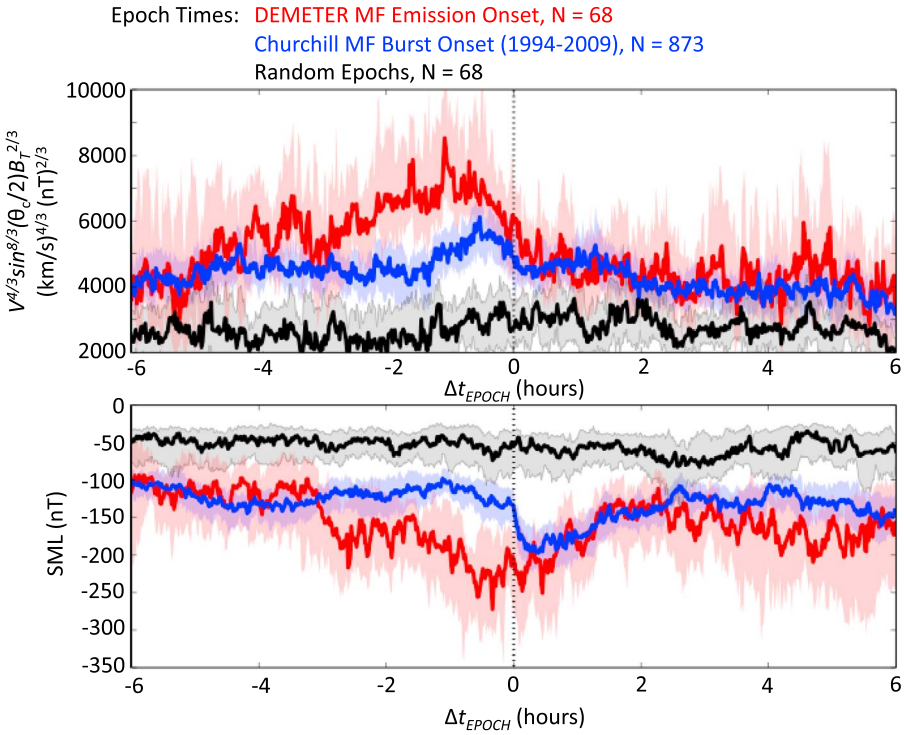

Figure 6. (top) A superposed epoch analysis of the solar wind hemispheric energy flux. (bottom) A superposed epoch analysis of the SML index. The lines represent the median value for three epoch times: Onset of the bursty MF waves observed by DEMETER (red), Onset of MF bursts observed at Churchill, Manitoba (blue), and random epochs (black). The shaded area is the bootstrapped 95% confidence interval on the median.

random population shows no effect. The SML index associated with Churchill MF bursts sharply decreases near the epoch time, consistent with observations of MF burst near local substorm onset [*LaBelle et al.*, 1997]. Similar to the SML index associated with Churchill MF bursts, the SML index associated with the DEMETER bursty MF waves is also below the level associated with random times, which suggests that the waves are associated with auroral activity. However, significant drops in the SML index value occur 1–3 h before the onset time of the bursty MF waves observed by DEMETER and persist through the epoch time.

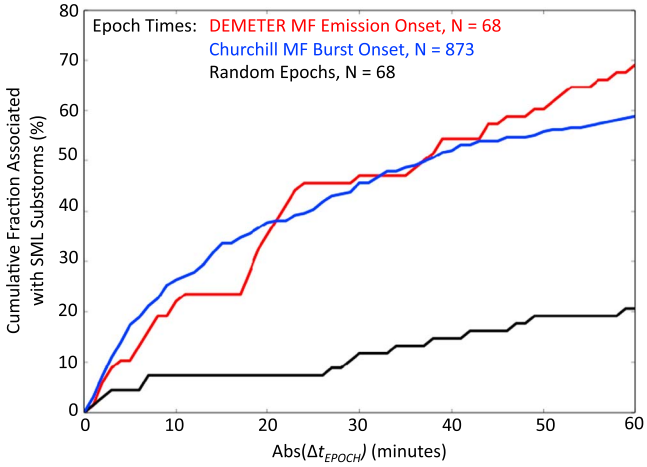

Figure 7. A plot of the cumulative fraction of epochs associated with SML-identified substorms for three populations: bursty MF waves observed by DEMETER (red), MF bursts observed at Churchill (blue), and random epochs (black).

The SuperMAG initiative also has a list of substorms that are identified by an automated algorithm [*Newell and Gjerloev*, 2011]. Figure 7 shows the cumulative fraction of epochs that are associated with an SML-identified substorm as a function of window size (Δt). Both positive and negative values of Δt were used. The slopes of the lines for the Churchill and DEMETER populations change to that of the random population after approximately $\Delta t = 20$ min, an indication that the events added to the cumulative fraction are those associated with an SML-identified substorm only by chance. From $0 < \Delta t < 20$ min, the cumulative fraction for both

©2014. American Geophysical Union. All Rights Reserved.

the Churchill and DEMETER populations exhibit similar behavior, which suggests that they both have a relationship to substorm onset.

4. Discussion

4.1. Relationship Between DEMETER MF Emissions and MF Burst

Ground level MF burst lasts for a few minutes during some substorm onsets. It is commonly observed just poleward of the expanding substorm aurora, and direction-finding observations suggest that it may originate from the poleward expanding arc, though propagation effects make these conclusions uncertain. Due to the short duration, the relatively infrequent occurrences of substorms at any given location and propagation effects that affect transmission to ground level, MF burst has a relatively low overall occurrence rate. A survey of 3886 nights of data from Churchill, Manitoba, spanning 1994–2008, reveals 873 observations of MF burst. The mean duration of an MF burst is approximately 10 min. MF bursts tend to be observed from 20 to 2 MLT [*LaBelle et al.*, 1997], so each day of data contains 36 ten minute intervals during which MF bursts would likely be observed at ground level. This yields an occurrence rate of 0.62% (873/(3886 × 36)). In the survey of DEMETER data, 8624 half orbits were examined, and bursty MF waves were identified on 66 separate half orbits, yielding an occurrence rate of 0.76% (66/8624). It is interesting that the occurrence rates are close in value despite differences in the data sets. First, the ground level observations were made at 69° invariant latitude, and for most half orbits DEMETER did not record data above 65° invariant latitude. Second, *D* region absorption has no effect on DEMETER observations but potentially a large effect on ground-level observations; for example, MF bursts that might be generated after local substorm onset may have been unable to propagate to ground level.

The strongest evidence for the hypothesis that the waves observed by DEMETER are MF bursts would be the simultaneous observation of waves in space and at ground level. Observations suggest that MF burst may propagate up to 300 km in ground distance from the source [*LaBelle et al.*, 2005]. Of the DEMETER half-orbits surveyed, 138 were within 300 km ground distance of either Churchill or Toolik Lake. The product of this number with the ground level occurrence rate gives the expected number of simultaneous MF burst observations by a ground level observatory and a satellite with DEMETER's orbit. Assuming perfect propagation to both ground level and to a satellite within 300 km ground distance of the ground level observation site, approximately one event is expected to be observed by both DEMETER and at ground level, which is consistent of our observation of only one event where similar waves were seen at the satellite and at ground level within a few minutes of each other.

In the single example of a nearly coincident event (Figure 3), the bursty MF waves observed by DEMETER occurred 7 min before Churchill observed MF burst. This delay could be explained by the approximately 1000 km spatial separation of the measurements combined with the spatiotemporal development of the auroral event. The source of the MF waves could have started near DEMETER's location and moved to a location where the MF waves could propagate subionospherically to Churchill. At the time the MF burst was observed at Churchill, magnetometers at Gillam, Island Lake, and Rabbit Lake showed decreases in the *H* component, which one would expect to see if a substorm onset were in progress on field lines south and west of Churchill. Gillam and Island Lake are located 270 km and 570 km south of Churchill, respectively. Rabbit Lake is located approximately 570 km west and slightly south of Churchill. Assuming the DEMETER observations originate from the source auroral event but at a ground distance 1000 km south and east of Churchill, the auroral event would have to propagate with speeds of 2.7 km/s, 2.4 km/s, and 4.3 km/s for propagation from DEMETER to Gillam, Island Lake, and Rabbit Lake, respectively. These velocities are close to the westward traveling surge velocities of 1–2 km/s reported by *Pytte et al.* [1976] and well within the range of westward traveling surge velocities, which can be as high as 30 km/s [*Opgenoorth et al.*, 1983]. Unfortunately, this motion could not be confirmed with optical data because of cloudy viewing conditions. The magnetometer and radio data are consistent with a westward traveling surge but are not conclusive.

A second, weaker, method to test the hypothesis that the waves observed by DEMETER are MF bursts would be to compare the wave characteristics observed in space and at ground level. Similar to MF burst, the bursty waves observed by DEMETER had an electric field amplitude around 100 μV/m, which falls into the 50–100 μV/m amplitude range of MF bursts observed at ground level [*LaBelle et al.*, 1997]. If MF waves are generated near the *F* peak or in the lower topside, the distance from their source to the ground is indeed approximately equal to the distance from their source to the DEMETER spacecraft. Depending on the generation mechanism, this similarity in the observed amplitudes appears coincidental, however, since waves

©2014. American Geophysical Union. All Rights Reserved.

observed in space and at ground level would presumably undergo different mode conversion processes. For example, in the mechanism proposed in *LaBelle* [2011], MF burst that propagates to ground level would first convert to *Z* mode waves and then to *O* mode waves. In contrast, the DEMETER MF waves would be the result of a direct conversion from the Langmuir to *O* mode waves at the location where the wave frequency matches the plasma frequency on the topside. Therefore, it seems somewhat coincidental, though not impossible, that the waves observed in space and at ground level would have the same amplitudes. Calculations beyond the scope of this paper are required to test the plausibility of that interpretation.

Both ground level MF burst and the DEMETER MF waves show a strong correlation with auroral hiss, a broadband, impulsive emission below f_{ce} having up to ~1 MHz bandwidth and few minutes timescale. The SML index associated with Churchill MF bursts decreased sharply near the MF burst onset time, an expected result since the waves were strongly associated with local substorm onset. The bursty MF waves observed with DEMETER are associated with depressed SML values, which is consistent with the idea that the waves are associated with strong auroral activity and substorms in some manner. However, a sharp drop in SML near the epoch time is absent as might be expected if the waves were strictly coincident with substorm onset. The difference between the two populations may be due to propagation effects that play a role in ground level observations of MF burst. Because of strong ionization of the lower regions of the ionosphere, radio waves in the MHz frequency range are strongly absorbed soon after substorm onset. Therefore, for a chain of multiple substorms, ground level observations are likely to see only MF bursts associated with the initial substorm onset, which suggests that the SML index would be relatively undisturbed prior to the appearance of MF burst at ground level. In situ observations would not show this bias. This may explain why the drop in the SML index tends to occur in the hours before MF waves are observed in space.

Orbital effects make it difficult to discern whether the MLT distribution of the waves observed by DEMETER is consistent with the hypothesis that the waves are MF burst. As can be seen in Figure 4c, the MLT distribution of MF bursts is distinct from the MLT distribution of the waves observed by DEMETER, even when the MF burst MLT distribution is convolved with the orbital MLT distribution of DEMETER. The orbital bias in invariant latitude reveals a complication, however. On a typical half orbit, DEMETER recorded data between only −65 and 65 invariant latitudes. Only 21% of the half orbits had data poleward 65° invariant; only 5% had data poleward of 68° invariant. Because of this, any auroral activity observed by DEMETER was likely to be the result of stronger solar wind driving, an idea that is consistent with the superposed epoch analysis of solar wind data shown in Figure 6 (top). As shown by the DMSP statistical studies of *Newell et al.* [2009], periods of stronger driving can lead auroral precipitation at earlier MLT, well into the evening sector, which would be consistent with the peak of DEMETER-observed MF waves near 18 MLT. However, without more events it is not possible to fully account for possible orbital biases in invariant latitude.

Ground level MF burst has been shown to be left-hand polarized [*Shepherd et al.*, 1997]. It also shows fine structure on the 100 ms time scale, such as the "backward seven" fine structure reported by *Bunch and LaBelle* [2009] and a direction of arrival that follows the motion of the poleward edge of an auroral arc [*Bunch et al.*, 2009]. Because the instrument on DEMETER measured only one component of the electric field at a relatively coarse time resolution, it was not possible to directly measure the polarization, fine structure, and direction of arrival of the bursty MF waves.

The power spectral density of the bursty MF waves shows a modulation at a period of approximately 15 s. MF burst has shown modulations that range from milliseconds to 30 s [*LaBelle et al.*, 1997]. Because the power spectral density modulation of MF burst has yet to be extensively characterized, it is difficult to assess whether the observations of modulation in the burst MF burst observed by DEMETER support or contradict the hypothesis that the waves are MF burst.

We can summarize the evidence for the hypothesis that the bursty MF waves observed by DEMETER are MF burst with the following:

1. A "backward seven" frequency fine structure on the time scale of 10–100 ms? N/A
2. A left-handed polarization? N/A
3. A direction of arrival that follows the motion of the poleward edge of an auroral arc? N/A
4. A broadband, impulsive frequency structure on the time scale of seconds and similar upper and lower frequency boundaries? Yes
5. An electric field amplitude of 50–100 μV/m? Qualified yes

©2014. American Geophysical Union. All Rights Reserved.

6. A strong correlation with auroral hiss? Yes
7. A strong correlation with substorm onset? Qualified yes
8. A magnetic local time distribution peaked in the premidnight sector? Unclear

In summary, the balance of the evidence suggests that the bursty MF waves observed with DEMETER are the same phenomenon as the ground level MF burst.

4.2. Implications of Topside Observations of MF Bursts

All proposed generation mechanisms of MF burst have focused on downward propagating radio waves. If the bursty MF waves observed by DEMETER are MF bursts, current proposed generation mechanisms that assume a source near the *F* peak would need to account for upward propagating waves as well. *LaBelle* [2011] proposed that MF bursts originate as Langmuir waves on the topside of the ionosphere. As they propagate downward, they reach a point where the wave frequency is equal to the local plasma frequency, allowing for mode conversion to the *Z* mode. A fraction of wave energy may convert to the *Z* mode and continue to propagate downward where under certain conditions it can propagate to ground level in the LO mode. At the topside mode conversion point, some of the Langmuir wave energy could be converted into upgoing *X* and *O* mode waves that could be observed at DEMETER's altitude. Using electron fluid simulations, *Kim et al.* [2008, 2013] studied this mode conversion in warm, magnetized plasmas and found that 50–99% of the wave power could be converted from the Langmuir mode to upgoing electromagnetic radiation. This mode conversion mechanism has yet to be studied in the ionospheric context, which should be the subject of future work.

An alternative source mechanism is suggested by the recent observations by radar and ground level radio instruments showing coincident MF burst and anomalous incoherent scatter radar echoes associated with strong Langmuir turbulence (SLT), suggesting that MF bursts may be a manifestation of the same mechanism that is thought to produce SLT in the *F* region of the ionosphere [*Akbari et al.*, 2013]. Once consequence of SLT is the formation of cavitons in the ionosphere, which in principle should radiate Langmuir waves both up and down the magnetic field line [*DuBois et al.*, 1990]. However, it is unclear if SLT could generate the ~1 MHz bandwidth of MF burst. Similar to the mechanism proposed by *LaBelle* [2011], mode conversion is needed for the waves to propagate to both ground level and satellite altitudes.

5. Conclusions

The DEMETER spacecraft observed bursty MF waves in the high-latitude topside ionosphere that are similar to auroral medium frequency bursts in amplitude, bandwidth, and occurrence rate. While we cannot state with certainty that the waves are MF bursts, much of the data are consistent with this hypothesis. Future observational work measuring the polarization and, if possible, the fine structure of these waves would help determine if they are MF burst. If the emissions are MF burst, they should be left-hand circularly polarized electromagnetic waves. They should also exhibit a fine structure similar to the "backward seven" fine structure of MF burst. Modeling efforts could estimate both the upgoing and downgoing mode conversion efficiencies of Langmuir waves to electromagnetic waves in the auroral ionosphere. For example, a model that attempts to both MF burst and the bursty MF waves observed by DEMETER should address the fact that the emissions have similar amplitudes, even though they may go through different mode conversion processes.Overall, these future observational and modeling efforts would help solve the mystery of both of these heretofore unexplained natural radio emissions.

Acknowledgments

The work of M.B. and J.L. was supported by National Science Foundation grant NSF AGS-1147699. For queries related to ground level radio data, please contact Jim LaBelle (jlabelle@aristotle.dartmouth.edu). The authors thank Xi Yan for her help with the survey of DEMETER data, Mike Trimpi for design of the SPR receiver, Hank Arjes for the design of the HF-2 radio receiver, Micah Dombrowski and Richard Brittain for software support, and the staff at the Churchill Northern Studies Center and Toolik Field Station for maintenance of the ground level radio equipment. The work of MP was supported by the Centre National dÕEtudes Spatiales. The authors thank J. J. Berthelier the PI of ICE for the use of the data. For queries related to DEMETER data, please contact Michel Parrot (michel.parrot@cnrs-orleans.fr). The authors thank I.R. Mann, D.K. Milling, and the rest of the CARISMA team for data. CARISMA is operated by the University of Alberta, funded by the Canadian Space Agency. CARISMA data are available at http://www.carisma.ca/. SuperMAG is made possible by the generous funding provided by the National Science Foundation (NSF) and National Aeronautics and Space Administration (NASA). We gratefully acknowledge: NSF ATM-0646323, NSF AGS-1003580, and NASA NNX08AM32G S03. SUPERMAG data are available at http://supermag.jhuapl.edu/.

Larry Kepko thanks the reviewers for their assistance in evaluating the paper.

References

Akbari, H., J. L. Semeter, M. J. Nicolls, M. Broughton, and J. W. LaBelle (2013), Localization of auroral Langmuir turbulence in thin layers, *J. Geophys. Res. Space Physics*, *118*, 3576–3583, doi:10.1002/jgra.50314.

Berthelier, J. J., et al. (2006), ICE, the electric field experiment on DEMETER, *Planet. Space Sci.*, *54*, 456–471, doi:10.1016/j.pss.2005.10.016.

Bunch, N. L. (2010), Ground based studies of auroral medium frequency burst radio emissions, PhD thesis, Dartmouth College, Hanover, N. H.

Bunch, N. L., and J. LaBelle (2009), Fully resolved observations of auroral medium frequency burst radio emissions, *Geophys. Res. Lett.*, *36*, L15104, doi:10.1029/2009GL038513.

Bunch, N. L., J. LaBelle, A. T. Weatherwax, and J. M. Hughes (2008), Auroral medium frequency burst radio emission associated with the 23 March 2007 THEMIS study substorm, *J. Geophys. Res.*, *113*, A00C08, doi:10.1029/2008JA013503.

Bunch, N. L, J. LaBelle, A. T. Weatherwax, J. M. Hughes, and D. Lummerzheim (2009), Experimental tests of the generation mechanism of auroral medium frequency burst radio emissions, *J. Geophys. Res.*, *114*, A09302, doi:10.1029/2008JA013993.

DuBois, D. F., H. A. Rose, and D. Russell (1990), Excitation of strong Langmuir turbulence in plasmas near critical density: Application to HF heating of the ionosphere, *J. Geophys. Res.*, *95*(A12), 21,221–21,272, doi:10.1029/JA095iA12p21221.

©2014. American Geophysical Union. All Rights Reserved.

Gjerloev, J. W. (2009), A global ground-based magnetometer initiative, *Eos Trans. AGU*, *90*(27), 230–231, doi:10.1029/2009EO270002.
Gurnett, D. A., S . D. Shawhan, and R. R. Shaw (1983), Auroral hiss, Z-mode radiation, and auroral kilometric radiation in the polar magnetosphere: DE-1 observations, *J. Geophys. Res.*, *88*, 329–340.
Kellogg, P. J., and S. J. Monson (1979), Radio emissions from the aurora, *Geophys. Res. Lett.*, *6*, 297–300, doi:10.1029/GL006i004p00297.
Kim, E., I. H. Cairns, and P. A. Robinson (2008), Mode conversion of Langmuir to electromagnetic waves at magnetic field-aligned density inhomogeneities: Simulations, theory, and applications to the solar wind and the corona, *Phys. of Plasmas*, *15*, doi:10.1063/1.2994719.
Kim, E., I. H. Cairns, and J. R. Johnson (2013), Linear mode conversion of Langmuir/z-mode waves to radiation in plasmas with various magnetic field strength, *Phys. of Plasmas*, *20*(12), 122103, doi:10.1063/1.4837515.
LaBelle, J. (2011), An explanation for the fine structure of MF burst emissions, *Geophys. Res. Lett.*, *38*, L03105, doi:10.1029/2010GL046218.
LaBelle, J., and R. A. Treumann (2002), Auroral radio emissions, 1. hisses, roars, and bursts, *Space Sci. Rev.*, *101*, doi:10.1023/A:1020850022070.
LaBelle, J., S. G. Shepherd, and M. L. Trimpi (1997), Observations of auroral medium frequency bursts, *J. Geophys. Res.*, *102*(A10), 22,221–22,231, doi:10.1029/97JA01905.
LaBelle, J., A. T. Weatherwax, M. Tantiwiwat, E. Jackson, and J. Linder (2005), Statistical studies of auroral MF burst emissions observed at South Pole Station and at multiple sites in northern Canada, *J. Geophys. Res.*, *110*, A02305, doi:10.1029/2004JA010608.
LaBelle, J., H. Dansu, N. L. Bunch, A. T. Weatherwax, E. L. Spanswick, and E. F. Donovan (2009), Substorm onsets at Churchill, Manitoba, inferred from radiowave emission data, Abstract SM41B-1731 paper presented at 2009 Fall Meeting, AGU.
Newell, P. T., and J. W. Gjerloev (2011), Evaluation of SuperMAG auroral electrojet indices as indicators of substorms and auroral power, *J. Geophys. Res.*, *116*, A12211, doi:10.1029/2011JA016779.
Newell, P. T., T. Sotirelis, K. Liou, C.-I. Meng, and F. J. Rich (2007), A nearly universal solar wind-magnetosphere coupling function inferred from 10 magnetospheric state variables, *J. Geophys. Res.*, *112*, A01206, doi:10.1029/2006JA012015.
Newell, P. T., T. Sotirelis, and S. Wing (2009), Diffuse, monoenergetic, and broadband aurora: The global precipitation budget, *J. Geophys. Res.*, *114*, A09207, doi:10.1029/2009JA014326.
Opgenoorth, H. J., R. J. Pellinen, W. Baumjohann, E. Nielsen, G. Marklund, and L. Eliasson (1983), Three-dimensional current flow and particle precipitation in a westward traveling surge (observed during the Barium-Geos Rocket Experiment), *J. Geophys. Res.*, *88*(A4), 3138–3152, doi:10.1029/JA088iA04p03138.
Parrot, M., U. S. Inan, N. G. Lehtinen, and J. L. Pinçon (2009), Penetration of lightning MF signals to the upper ionosphere over VLF ground-based transmitters, *J. Geophys. Res.*, *114*, A12318, doi:10.1029/2009JA014598.
Pytte, T., R. L. McPherron, and S. Kokubun (1976), The ground signatures of the expansion phase during multiple onset substorms, *Planet. Space Sci.*, *24*(12), 1115–1132, doi:10.1016/0032-0633(76)90149-5.
Qin, Z., R. E. Denton, N. A. Tsyganenko, and S. Wolf (2007), Solar wind parameters for magnetospheric magnetic field modeling, *Space Weather*, *5*, S11003, doi:10.1029/2006SW000296.
Rothkaehl, H. (1999), HF plasma emission detected in the cusp region at ionospheric altitude, *Adv. Space Res.*, *23*(10), 1769–1772, doi:10.1016/S0273-1177(99)00387-7.
Sato, Y., T. Ono, M. Iizima, A. Kumamoto, N. Sato, A. Kadokura, and H. Miyaoka (2008), Auroral radio emission and absorption of medium frequency radio waves observed in Iceland, *Earth Planets Space*, *60*, 207–217.
Shepherd, S. G., J. LaBelle, and M. L. Trimpi (1997), The polarization of auroral radio emissions, *Geophys. Res. Lett.*, *24*(24), 3161–3164, doi:10.1029/97GL03160.
Shutte, N., I. Prutensky, S. Pulinets, Z. Klos, and H. Rothkaehl (1997), The charged-particle fluxes at auroral and polar latitudes and related low-frequency auroral kilometric radiation-type and high-frequency wideband emission, *J. Geophys. Res.*, *102*(A2), 2105–2114, doi:10.1029/96JA01116.
Weatherwax, A. T. (1994), Ground-based observations of auroral radio emissions, PhD thesis, Dartmouth College, Hanover, N. H.
Weatherwax, A. T., J. LaBelle, and M. L. Trimpi (1994), A new type of auroral radio emission observed at medium frequencies (1350–3700 kHz) using ground-based receivers, *Geophys. Res. Lett.*, *21*(24), 2753–2756.

©2014. American Geophysical Union. All Rights Reserved.